Journal of Engineering Science and Technology Review 11 (2) (2018) 72 - 81

Research Article

JOURNAL OF
Engineering Science and Technology Review

www.jestr.org

Experimental Observation of Antimonotonicity in a Nonlinear R-L-Diode Circuit

P. A. Daltzis*,[1], N. A. Gerodimos[1], C. K. Volos[2], H. E. Nistazakis[1] and G. S. Tombras[1]

[1]Department of Electronics, Computers, Telecommunications and Control, Faculty of Physics, National and Kapodistrian University of Athens, Athens, 15784, Greece

[2]Laboratory of Nonlinear Systems, Circuits & Complexity (LANSCOM), Department of Physics, Aristotle University of Thessaloniki, Thessaloniki, GR-54124, Greece.

Received 22 November 2017; Accepted 25 March 2018

Abstract

In this work the antimonotonicity phenomenon is experimentally investigated in the case of a driven nonlinear R-L-Diode circuit, with or without a DC bias voltage. The nominated electronic circuit is one of the simplest and extensively studied nonlinear circuits that can be made in breadboard. Due to this fact, this is not an introductory paper but focuses specifically to the study of how the frequency of the sinusoidal voltage source acts to the dynamical behavior of the circuit, using appropriate nonlinear tools such as the bifurcation diagram, phase portrait, return map and correlation dimension. Furthermore, except of the antimonotonicity, a number of other interesting phenomena related to chaos has also been observed.

Keywords: Chaos, antimonotonicity, nonlinear circuit, bifurcation diagram, phase portrait, return map, correlation dimension.

1. Introduction

During the last decades, the fact that several nonlinear electronic circuits exhibit chaotic behavior has attracted the interest in the academic and industrial community. This fact has led in observing in electronic circuits, chaotic phenomena [1] that have been reported in literature, such as well-known routes to chaos, period doubling and intermittency, quasiperiodicity route to chaos, crisis and antimonotonicity [2-7]. Today, due to the introduction of digital oscilloscopes, those effects can be accurately depicted utilizing computer data analysis without the need of complex triggering systems.

The sinusoidally driven Resistor-Inductor Diode (RLD) circuit, due to its simplicity is one of the most extensively studied electronic circuits presenting complex dynamics. The proposed non-autonomous circuit consists of a p-n junction diode in series with an inductor and a resistor, which presents nonlinear dynamic behavior and exhibits chaotic phenomena at higher input frequencies of the voltage source than other nonlinear electronic circuits do. Due to this fact, the RLD circuit can be used as a simple yet powerful tool for understanding possible chaos applications in random numbers generators, encryption and secure communication schemes. Also, regarding the investigation of chaotic behavior in the RLD circuit, many different approaches can be distinguished, focusing not only on the exploration and understanding of its chaotic properties but also to the reason why such nonlinear effects, are present [8, 9].

Antimonotonicity is a fundamental phenomenon in bifurcations for a large class of nonlinear dissipative systems, where periodic orbits are not only created but also destroyed, as a control parameter of the system increases in a monotone way. As an example of a system depicting period doubling route to chaos is the logistic map $x_{n+1} = rx_n(1-x_n)$. As the parameter r in that map increases, monotone behavior in the sense that the created periodic orbits are never destroyed [10] can be noticed. On the other hand, a nonlinear dynamical system can depict not only a monotone period doubling route to chaos but can also depict a reverse bifurcation sequence where periodic orbits are not only created but also destroyed [11]. Antimonotonicity was the name given by Dawson *et. al.* in [12] to the above chaotic phenomenon that can be found both in two dimensional systems [11, 13] and one dimensional maps [12,14]. Moreover, since one-dimensional maps must be noninvertible for chaotic dynamics to occur, it is more difficult to rigorously establish a conclusion concerning antimonotonicity for a one dimensional map than it is for a two-dimensional one. In the two dimensional case antimonotonicity is related with the homoclinic tangency of a periodic point. In higher scalar maps, Dawson *et. al.* in [15] introduced the dimple formation geometrical mechanism to explain the phenomenon. More general, Bier and Bountis [16] stated that the necessary condition for the antimonotonicity to occur in any nonlinear system is the state equations invariance under an existent symmetry transformation in the system. Moreover, it has been shown in [17] that the variation of two parameters in a nonlinear system is indicative for the system that inverse period doublings will be presented. A general form of a bifurcation diagram depicting the phenomenon of antimonotonicity, while a control parameter of the system is varying in a monotonous way, is shown in Fig. 1. In the "period-*N* chaotic bubble" case the system leaves the period *N* state following the route to chaos with period doublings. After the chaotic regime it ends again in the period-*N* state having followed reverse period doublings.

*E-mail address: pdaltzis@phys.uoa.gr
ISSN: 1791-2377
doi:10.25103/jestr.112.11

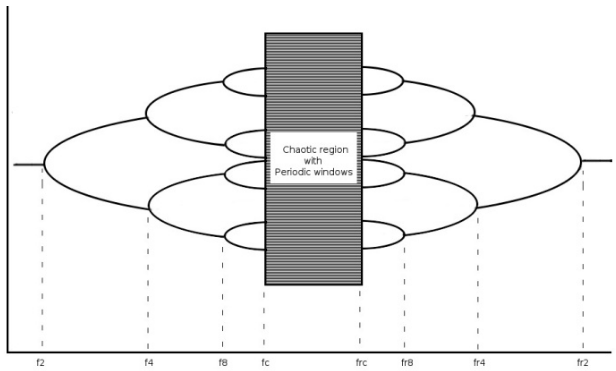

Fig. 1. Period $N = 1$ chaotic bubble.

In this paper, the experimental study of the RL-Diode circuit not only confirms the above work, but also extends the investigation of the RLD dynamic behavior regarding antimonotonicity. Using the frequency of the input signal as a control parameter of the system, bifurcation diagrams are constructed in order the antimonotonicity to be revealed.

The paper is organized as follows. Section 2 provides a brief description of the RL-Diode circuit, which is used in this work. In Section 3 the experimental results of the confirmation of the antimonotonicity phenomenon in the proposed circuit with and without a DC bias voltage are presented. Finally, the conclusive remarks are drawn in the last Section.

2. RLD Circuit Description

The schematic diagram of the resistor–inductor–diode (RLD) circuit used in this work, in order to investigate the phenomenon of antimonotonicity, is presented below in Fig. 2.

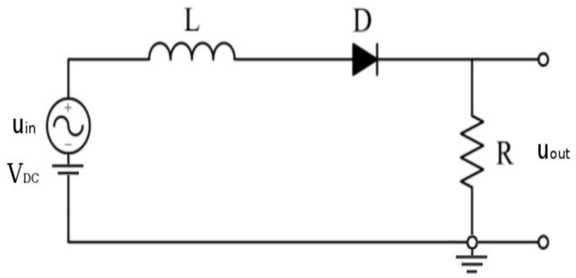

Fig. 2. RLD chaotic oscillator.

The circuit consists of a linear resistor R, in series with a linear inductor L and a diode D driven by an AC-voltage source $\upsilon_{in} = V_{in}\sin(\omega t)$. Diode type is 1N4005 and is the only nonlinear circuit element. The input signal is a sinusoidal voltage υ_{in} with frequency f_{in}, while υ_{out} is the output voltage of the signal across the resistor R. The element values chosen for R, L and D in each case are not chosen in random. They have been picked by try and error method using a digital oscilloscope connected at υ_{in} and υ_{out} terminals and observing the Lissajous curves generated by altering the amplitude υ_{in}. When circuit is not in chaotic state, Lissajous curves generated are stable indicating that between input and output, only a time delay of some sort occurs (Fig. 3). As the input voltage is altered monotonically, Lissajous curves reveal how period doubling bifurcations and reversals look on an oscilloscope screen (Fig. 3).

To the trained eye, when Lissajous curves start to get wobbly, this is an indication of a possible chaotic operation. A strong argument to support this is that since Lissajous curves are constructed by υ_{in} and υ_{out} and υ_{in} is always a smooth sinusoidal waveform, "wobbliness" is generated by υ_{out}, dictating that υ_{out} has become aperiodic. Of course, there is a need to examine the υ_{out} time series for the presence of chaos. In order to do that the appropriate time series is captured by taking account of the "wobbliness" of the constructed Lissajous curves. This surprisingly helpful property of the Lissajous curves dictates that they must be some sort of phase space projection to a plane. To verify this, we must depict the system's dynamics. In order to do that we use the diode's model proposed in [18], where the nonlinear element is considered as a nonlinear capacitor in parallel with a nonlinear resistor. For that purpose the characteristic i-υ curve of the specific diode is used in order to determine the nonlinear resistance. Nonlinear capacitive properties of the diode are derived from the properties of the semiconductor material of the diode when an ac signal acts to the transport carriers causing recombinations around the p-n junction, revealing chaotic behavior in specific conditions.

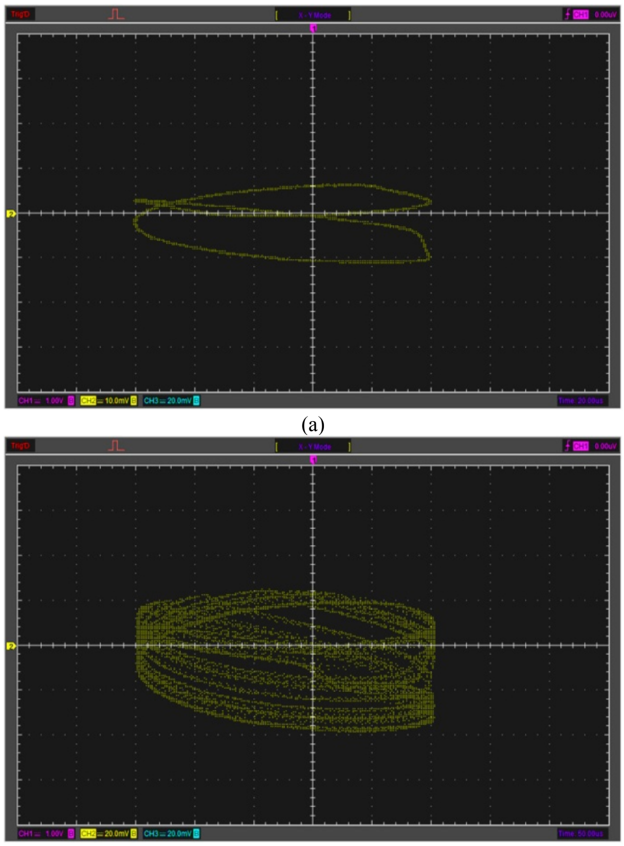

(a)

(b)

Fig. 3. Lissajous curves υ_{in} vs. υ_{out} for (a) period-2 operation and (b) for chaotic operation.

By applying Kirchoff's laws to the circuit of Fig. 2 the following dimensionless equations are derived.

$$\begin{cases} \dfrac{\mathrm{d}x}{\mathrm{d}\tau} = B\sin(\tau) + y - \dfrac{x}{\beta} \\ \dfrac{\mathrm{d}y}{\mathrm{d}\tau} = G(x,y) \end{cases} \tag{1}$$

where

$$G(x,y) = \begin{cases} \dfrac{x - \gamma\left(e^{\alpha y} - 1\right)}{c_1\left[e^{\alpha y} + c_2\left(1-y\right)^{-m}\right]}, & if \quad y < \dfrac{1}{2} \\ \dfrac{x - \gamma\left(e^{\alpha y} - 1\right)}{c_1\left[e^{\alpha y} + c_2^{\frac{(b_2+my)}{b_1}}\right]}, & if \quad y \geq \dfrac{1}{2} \end{cases} \tag{2}$$

The variables in system (1) are: $x = i\omega L/V_J$, $y = \upsilon/V_J$, where i and υ are the current in the RLD circuit and the voltage across the diode D respectively. Also, $\tau = \omega t$ and V_J is the junction potential. Furthermore, Eqs. (1) and (2) parameters are: $B = V_{in}/V_J$, $\beta = \omega L/R$, $\alpha = eV_J/(nkT)$, $\gamma = \beta I_S R/V_J$, $c_1 = R\beta\omega C_0$, and $c_2 = C_b/C_0$, where C_b is the zero voltage bias capacitance. $C_d = C_0\exp(eV/nkT)$ is a second capacitive effect arises when the finite response time of the mobile charges to the changing field is considered.

3. Experimental Observation of Antimonotonicity

In this section, the experimental observation of the antimonotonicity phenomenon is studied in two different cases. In the first one the classical R-L-Diode circuit, which was described in the previous section, is studied regarding the aforementioned phenomenon. For this reason, by keeping constant the values of circuit's resistance and impedance, bifurcation diagrams of voltage across the resistor (υ_{out}) versus the frequency (f) of the sinusoidal voltage source, is produced, for various values of source's amplitude V_{in}. In the same way, by adding a DC bias voltage V_{DC} in series with the other circuit's elements (Fig. 2), the antimonotonicity phenomenon is experimentally investigated again for different values of the DC source's value V_{DC}.

Our experimental setup shown in Fig. 4 is composed of a 1N4005 silicon rectifier diode, an 8.5 mH inductor with an internal resistance of 20 Ω and a resistor R in series with the inductor and the diode. In the no DC bias voltage case, a resistor R = 330 Ω is used, which is substituted by an R = 80 Ω resistor in the DC bias case. The resonator is driven by an arbitrary waveform generator. The output of the generator is buffered from the resonator input using an LF356N op-amp. The voltage drop across the resistor is collected by an oscilloscope probe and is digitized by the oscilloscope with 8 bit vertical resolution at 200 Msamples/sec. A computer is used to control both the waveform generator and the digital oscilloscope and also to acquire and process the generated data.

In order to increase the vertical resolution of the digitized signal, oversampling and decimation of the voltage drop across the 330Ω resistor are executed. Oversampling and decimation is a common method of increasing vertical resolution in modern digital oscilloscopes but here, instead of digital signal processing, a computer script is used for designation. This way, 10 bit vertical resolution, which helps in the true maxima approximation of time-series, is achieved. The time-series, is then processed using TISEAN package [19] in order to locate the local maxima that will be used to plot the bifurcation diagrams and return maps presented below.

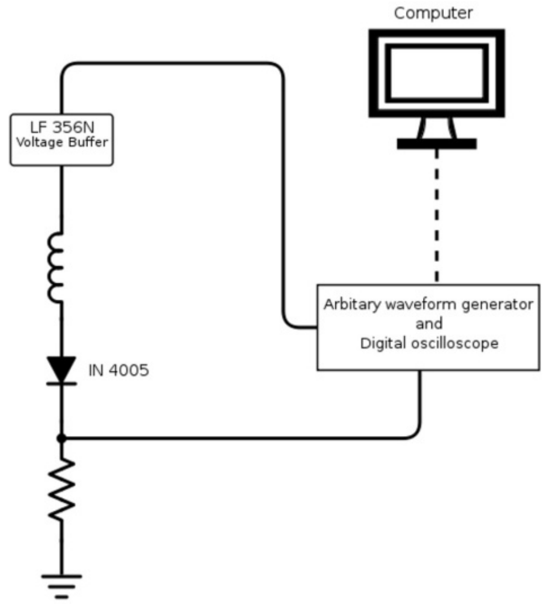

Fig. 4. Experimental setup.

3.1 Antimonotonicity in the R-L-Diode Circuit Without a DC Bias Voltage

By keeping constant the circuit's parameters R = 330 Ω, L = 8.5 mH and diode 1N4005, as illustrated in Fig. 2 the dynamic behavior of the circuit is investigated. Bifurcation diagrams of the maxima of voltage (V_{out}) across the resistor versus the frequency (f) of the sinusoidal voltage source, for various values of source's amplitude (V_{in}), are shown in Fig. 5.

At low values of amplitude (V_{in}) the circuit is always in period-1 steady state and as a consequence it never bifurcates, as it is shown in Fig.5(a), for V_{in} = 0.8 V. For these values of drive amplitude (V_{in}) the diode is predominantly reverse biased and essentially acts as a high impedance device. However, as the value of amplitude (V_{in}) increases period doubling bifurcations occur and the antimonotonicity phenomenon begins to form. In Fig. 5(b) an example of a *period-8 bubble* is displayed, for V_{in} = 2.1 V. Specifically, by constructing the relative bifurcation diagram, the scheme period-1 → period-2 → period-4 → period-8 → period-4 → period-2 → period−- is revealed. Furthermore, in Fig. 5(c) the cascades continue with the appearance of two *period-2 bubbles* at V_{in} = 2.4 V, in each one of the two main branches in the region of $f \in$[180 kHz, 290 kHz]. Therefore, for low values of drive amplitude (V_{in}) a series of forward and inverse bifurcations occur in frequency bands, which are increased with the increasing of the amplitude (V_{in}). These kind of periodic bubbles have been observed in many other systems, such as discrete maps [20] and circuits [21].

Figures 5(d)-(f) display the accumulation of bubbling that has led to the chaotic bands. In more details, for V_{in} = 2.7 V, as it can be shown in the bifurcation diagram of Fig. 5(d), a visible period doubling sequence leads the system to a chaotic region for $f \in [185$ kHz, 280 kHz$]$ and then an inverse period doubling sequence drives the system back to the initial period-1 steady state. In this way the well-known *period-1 chaotic bubble* has been configured. By increasing the value of amplitude (V_{in}) the chaotic bands expand as illustrated in Fig. 5(e) and Fig. 5(f). Also, phenomena related with chaos theory are also observed, such as a tangent bifurcation [22], which latches the circuit into a period-3 region, and the hysteresis phenomenon [23], which is explained as a result of the intersection of the unstable trajectory of period-3 with the chaotic attractor. So, as the amplitude (V_{in}) increases, a more complicated circuit's dynamic behavior is observed in a wider range of frequency.

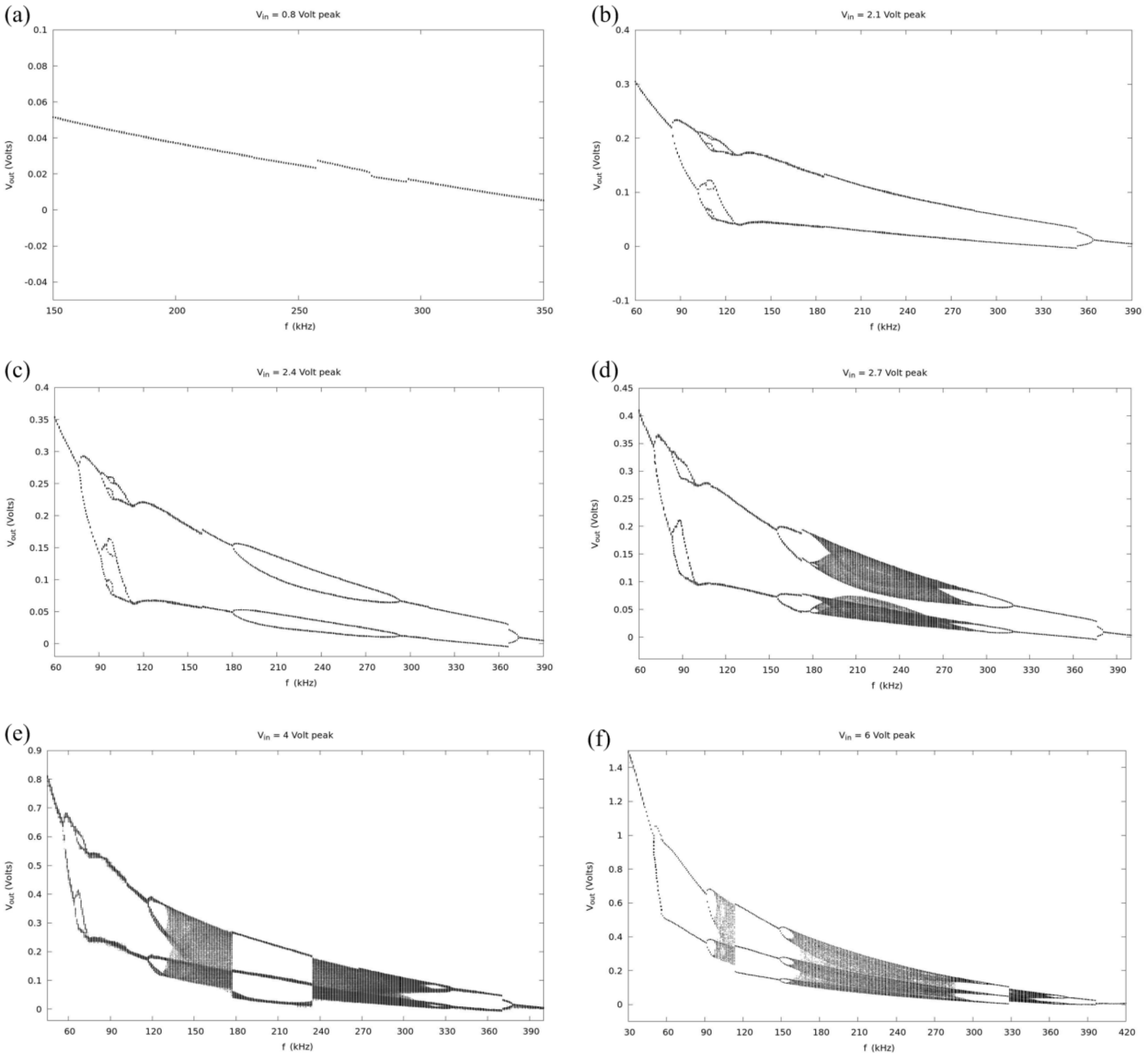

Fig. 5. Experimental bifurcation diagrams of voltage (V_{out}) versus frequency (f) of the circuit of Fig. 2, for R = 330 Ω, L = 9.5 mH and (a) V_{in} = 0.8 V, (b) V_{in} = 2.1 V, (c) V_{in} = 2.4 V, (d) V_{in} = 2.7 V, (e) V_{in} = 4 V and (f) V_{in} = 6 V.

3.2 Antimonotonicity in the R-L-D Circuit with a DC Bias Voltage

In this section, the R-L-Diode circuit's dynamic behavior in regards to the signal of a DC bias voltage is studied. Figure 6 displays the bifurcation diagram of the maxima of the voltage across the resistor (V_{out}) versus the signal of the DC voltage source (V_{DC}), for R = 80 Ω, L = 9.5 mH, V_{in} = 2.5 V and f = 180 kHz. A *period-1 chaotic bubble* has been configured, as the signal of the DC voltage source (V_{DC}) increases in the range $V_{DC} \in [-1$ V, 0.5 V$]$. In more details, the circuit commences with a period-1 limit cycle for $V_{DC} = -1$V. Then, the circuit undergoes a visible period doubling route to a chaotic region, which is interrupted by windows of periodic behavior. As the value of the signal V_{DC} further increases the system enters to a period-2 region. Another period doubling cascade commences when $V_{DC} = -0.115$ V. This cascade continues into a chaotic regime. At $V_{DC} = 0.069$ V, a tangent bifurcation occurs latching the circuit into a period-3 region. A period-6 steady state is subsequently born at V_{DC} = 0.155 V. So, forward period doubling bifurcations drive the circuit into a chaotic region, from which it exits to a period−1 state at V_{DC} = 0.408 V with inverse period doublings

.

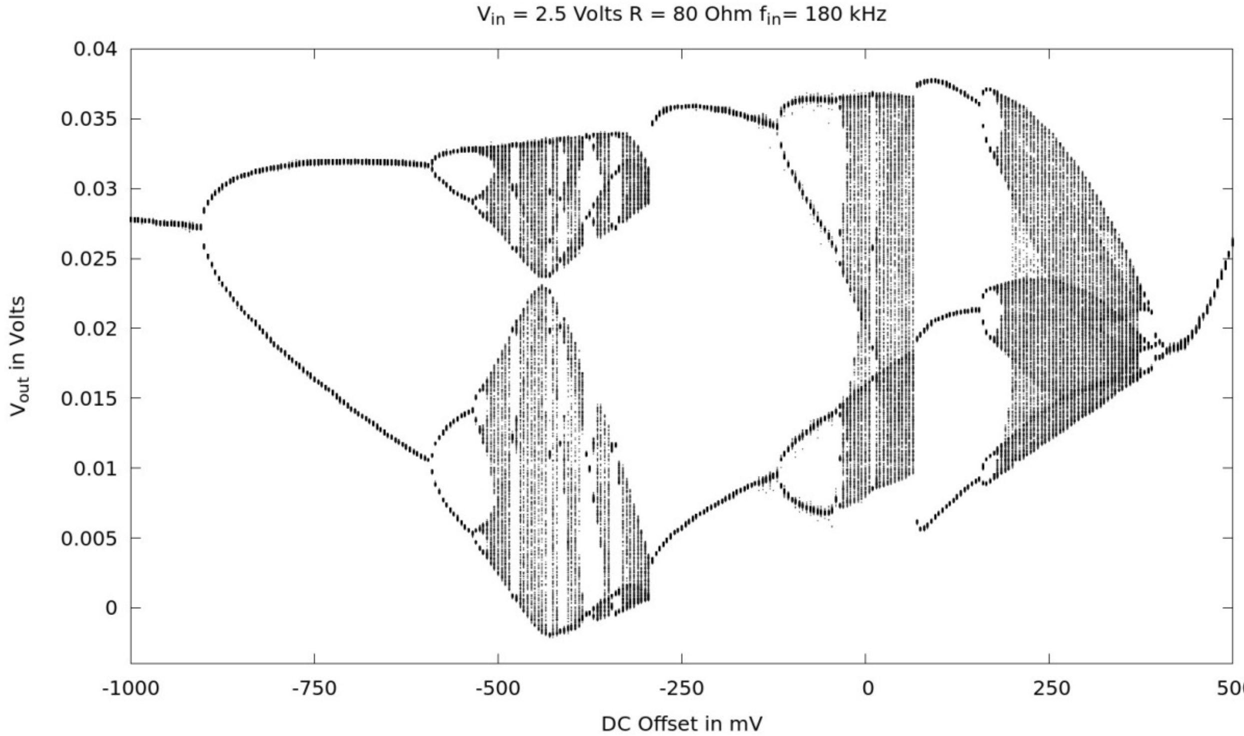

Fig. 6. Experimental bifurcation diagram of voltage (V_{out}) versus the signal of the DC voltage source (V_{DC}), of the circuit of Fig. 2, for R = 80 Ω, L = 9.5 mH, V_{in} = 2.5 V and f = 180 kHz.

By choosing various values of the signal of the DC bias voltage (V_{DC}), in the range of $V_{DC} \in [-1$ V, 0.5 V], a series of bifurcation diagrams of the voltage (V_{out}) versus the frequency (f) of the sinusoidal voltage source are captured (Fig. 7). At low values of the DC bias voltage (V_{DC}) the circuit is always in period-1 steady state and as a consequence it never bifurcates, as it is shown in Fig. 7(a), for V_{DC} = −1 V. However, as the value of the DC bias voltage (V_{DC}) increases, period doubling bifurcations occur and the antimonotonicity phenomenon begins to form. In Fig. 7(b) an example of a period-2 bubble, which is also called as primer bubble [50], is displayed for V_{DC} = −0.6 V, while in Fig. 7(c) a period−4 bubble is illustrated for V_{DC} = −0.55 V. Furthermore, in Fig. 7(d) the cascades continue with the appearance of a period-8 bubble at V_{DC} = −0.51 V, as well as a third period doubling in each one of the two main branches in the region of $f \in$[173.33 kHz, 221.60 kHz] is displayed.

Therefore, for low values of the DC bias voltage (V_{DC}) a series of forward and inverse bifurcations occurs again in frequency bands, which increase with the increasing of the DC bias voltage (V_{DC}). Figures 7(e) - (g) display the accumulation of bubbling that has led to the chaotic bands. In more details, for V_{DC} = −0.5 V, in the case of the bifurcation diagram of Fig. 5(e), a visible period doubling sequence leads the system to a chaotic region for $f \in$ [169.74 kHz, 205.92 kHz] and then inverse period doubles driven the system back to initial period-1 steady state. So, in this way a period-1 chaotic bubble has been configured. The expansion of the chaotic bands is illustrated in Fig. 7(f) - (g), as the value of amplitude (V_{DC}) increases. Also, phenomena related to chaos theory are also observed, such as a tangent bifurcation [22], which latches the circuit into a period-3 region, and the hysteresis phenomenon [23]. So, as the DC bias voltage (V_{DC}) increases, a more complicated circuit's dynamic behavior is observed in a wider range of frequency.

Experimental phase portraits of (υ_{out}) versus (υ_{in}) for different amplitude values of input voltage signal (V_{in}) are illustrated in Fig. 8. Also, the experimental first return maps of $V_{max}(n + 1)$ versus $V_{max}(n)$, can be shown respectively in the same figure, by keeping constant the value of R = 80 Ω, L = 9.5 mH, V_{in} = 2.5 V and V_{DC} = −0.45 V, for various values of frequency. From the aforementioned figure the forward and inverse bifurcations is confirmed as it is expected according to the bifurcation diagram of Fig. 7(f), for the chosen value of V_{DC} = −0.45 V. Furthermore, the folding of the attractor in the (υ_{in}, υ_{out})-plane, as the frequency increases, has been illustrated in Fig. 8.

This is a good point to investigate the presence of chaos in the time series collected, in order to plot Fig. 8(d). The investigation uses the correlation dimension which is calculated by the delay vector reconstructed attractor through analysis using TISEAN [19] according to [24]. Correlation dimension d is the invariant measure of dimensionality of the space occupied by random points and is a type of fractal dimension of the strange attractor. As it is described in [24], the correlation sum local slopes for different values ε and m in x-axis log scale is plotted and illustrated in Fig. 10, in order to verify the existence of a plateau with constant scaling exponent in a scale range, for all embedding dimensions larger than $m_{\min} > D$. As it can be seen the curves in the plateau of the above Fig. 10 are flat and are also collapsed for a wide range of length scales in x-axis, indicative that there is no (e, m) dependence for $m > m_{\min}$. From nonlinear time series analysis theory this scaling exponent is thus the appropriate parameter in order to estimate the correlation dimension of the system attractor. To estimate correlation dimension, we plot the double logarithmic plot of $C(m, \varepsilon)$ versus ε (Fig. 11). Then a function $f(x) = ax^b$ is fitted in the linear part of the double logarithmic plots, where $C(\varepsilon)$ follows a power law as it is described in [24]. The correlation dimension calculated using the aforementioned steps is D = 2.09, thus RLD circuit is producing a chaotic time series.

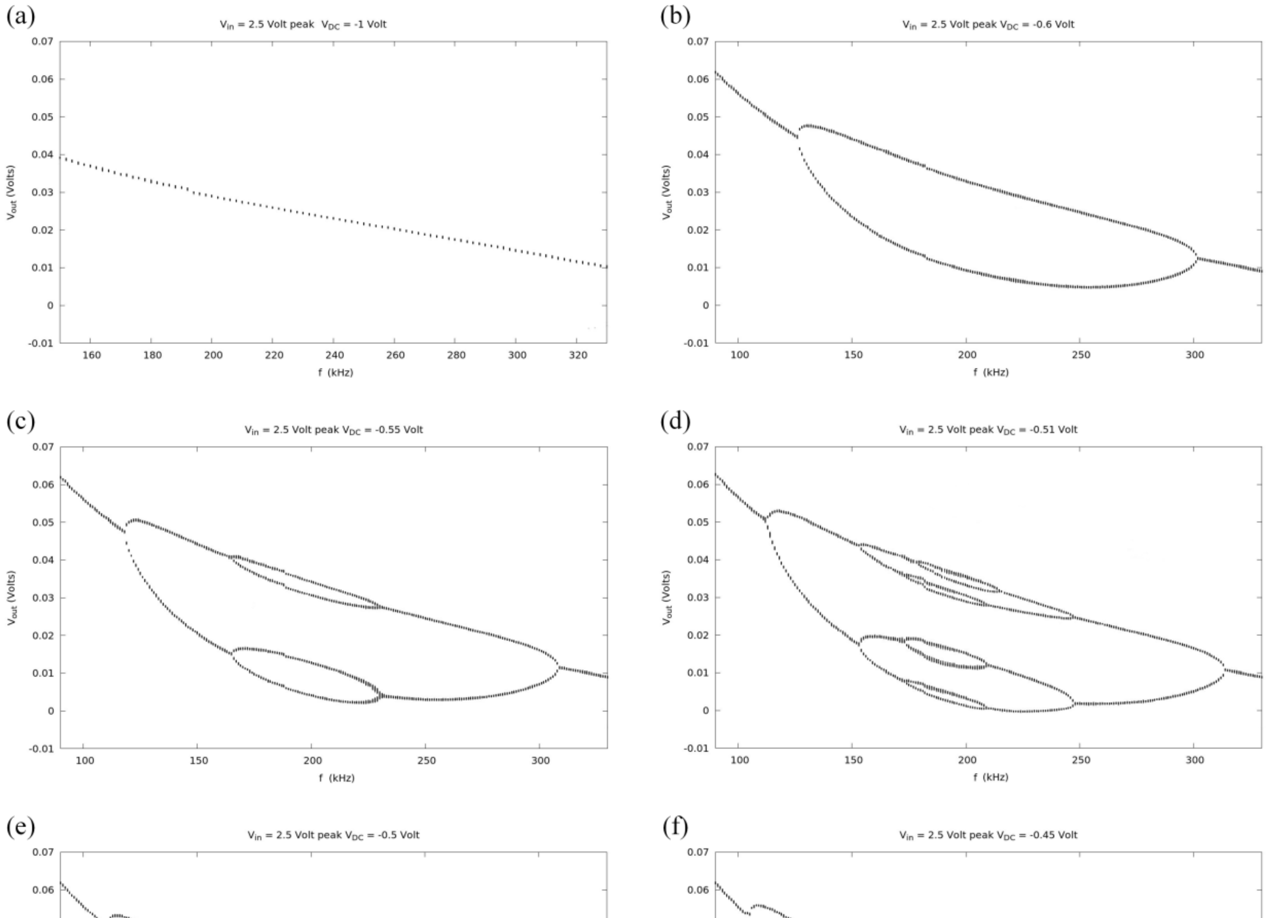

Fig. 7. Experimental bifurcation diagrams of voltage (V_{out}) versus frequency (f) of the circuit of Fig. 2, for R = 80 Ω, L = 9.5 mH, V_{in} = 2.5 V and (a) V_{DC} = -1 V, (b) V_{DC} = -0.6 V, (c) V_{DC} = -0.55 V, (d) V_{DC} = -0.51 V, (e) V_{DC} = -0.50 V, (f) V_{DC} = -0.45 V, (g) V_{DC} = 0 V and (h) V_{DC} = 0.25 V.

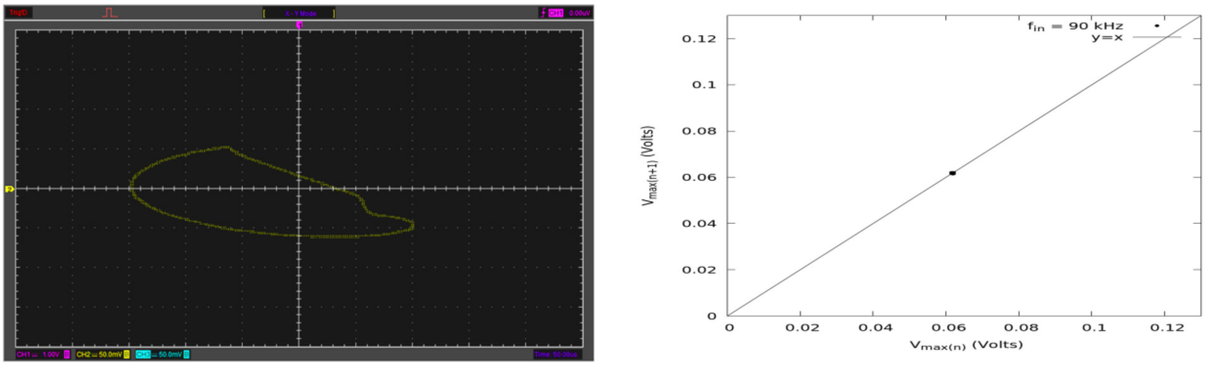
fin = 90 kHz
y=x
Vmax(n) (Volts)
Vmax(n+1) (Volts)

(a)

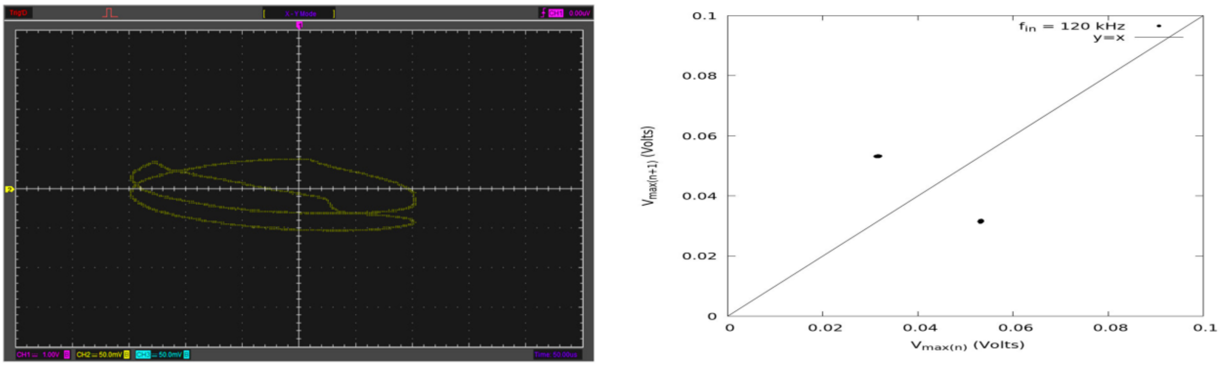
fin = 120 kHz
y=x
Vmax(n) (Volts)
Vmax(n+1) (Volts)

(b)

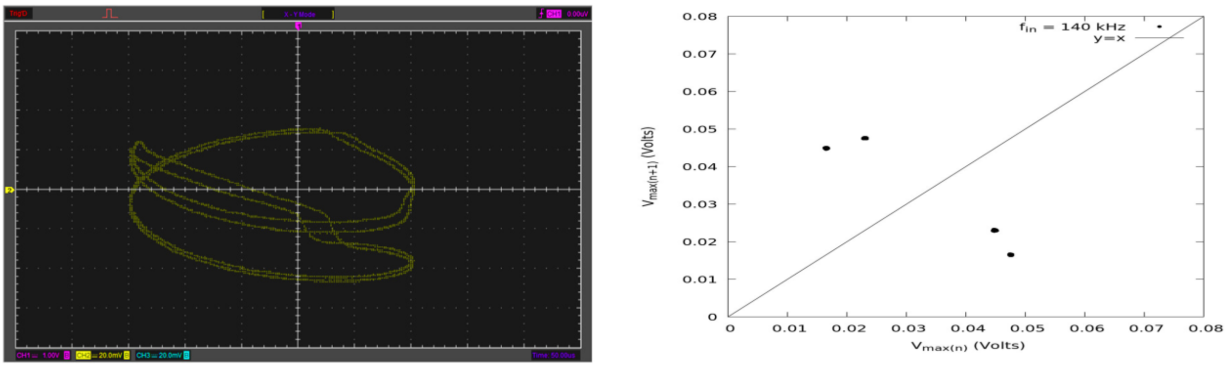
fin = 140 kHz
y=x
Vmax(n) (Volts)
Vmax(n+1) (Volts)

(c)

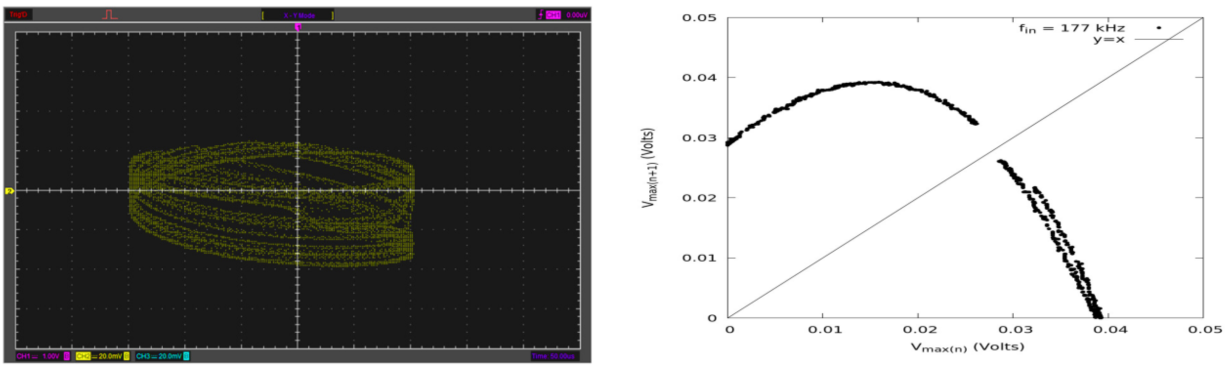
fin = 177 kHz
y=x
Vmax(n) (Volts)
Vmax(n+1) (Volts)

(d)

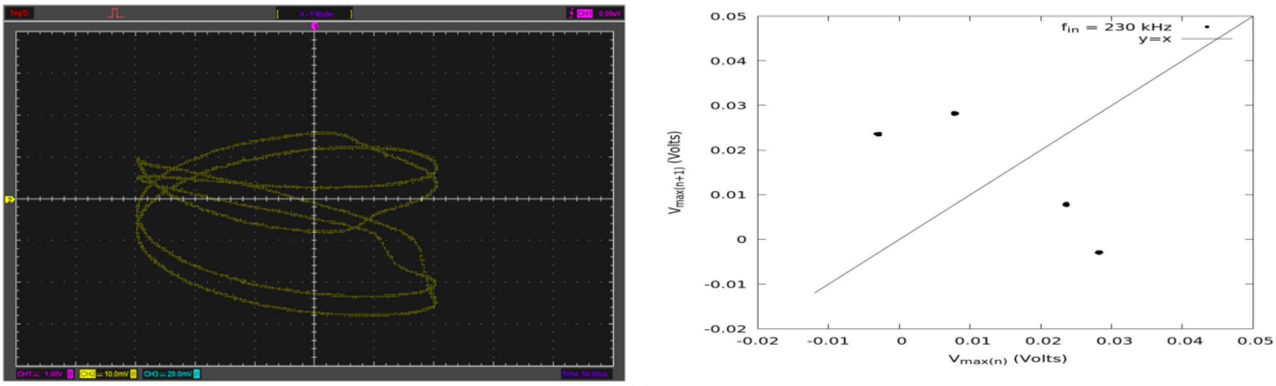

(e)

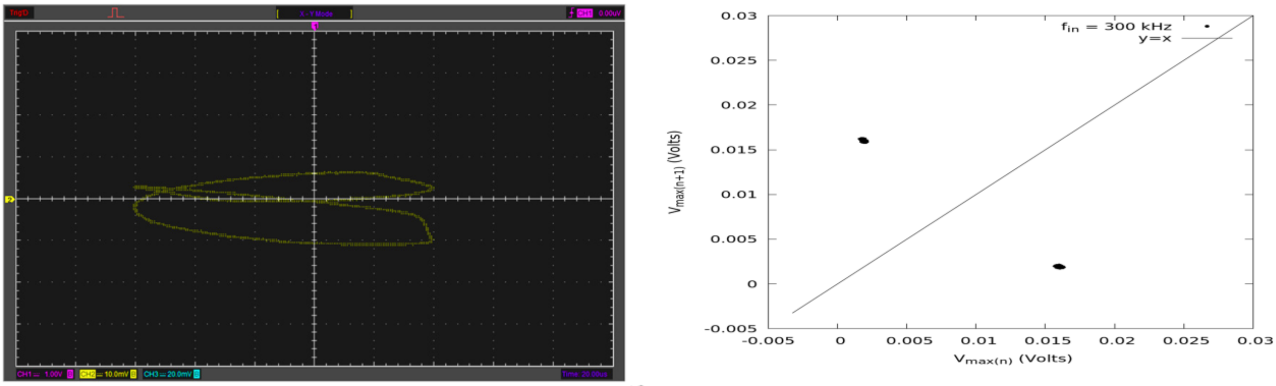

(f)

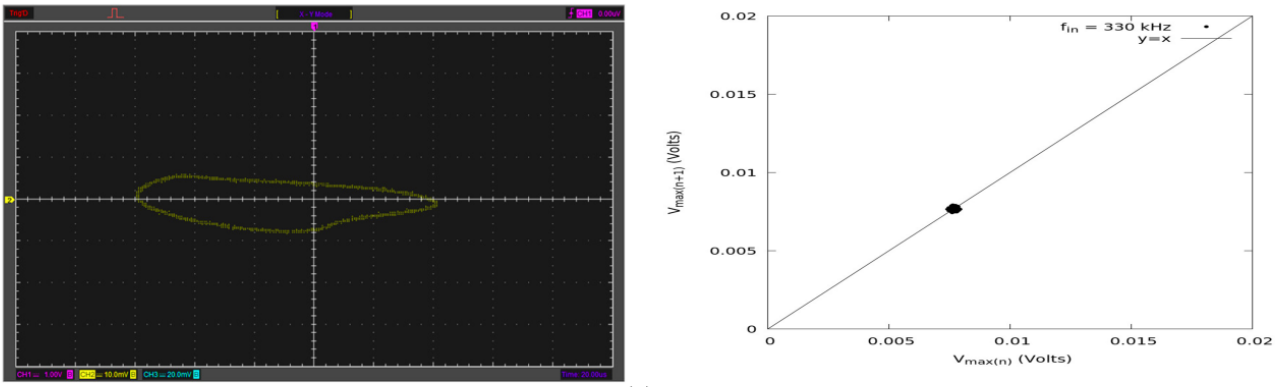

(g)

Fig. 8. Experimental phase portraits of (υ_{out}) versus (υ_{in}) and the respective experimental return maps of $V_{\max}(n+1)$ versus $V_{\max}(n)$, for R = 80 Ω, L = 9.5 mH, V_{in} = 2.5 V, V_{DC} = -0.45 V and (a) f = 90 kHz (period-1), (b) f = 120 kHz (period-2), (c) f = 140 kHz (period-4), (d) f = 177 kHz (chaos), (e) f = 230 kHz (period-4), (f) f = 300 kHz (period-2) and (g) f = 330 kHz (period-1).

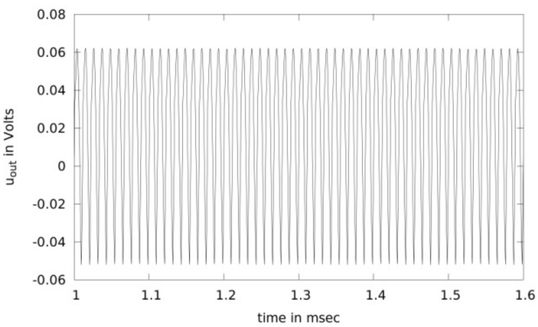

(a)

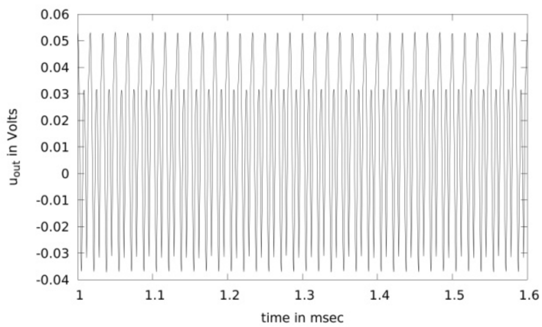

(b)

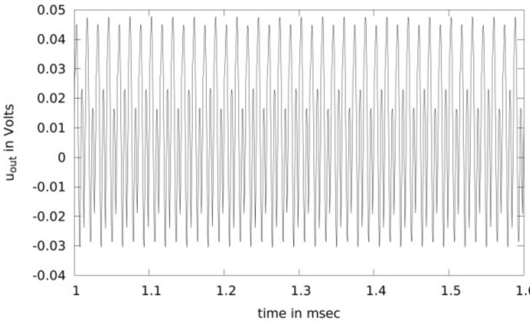

(c)

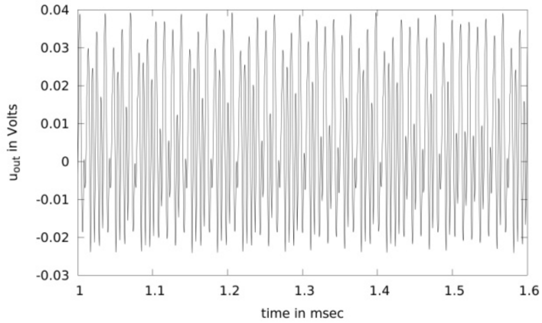

(d)

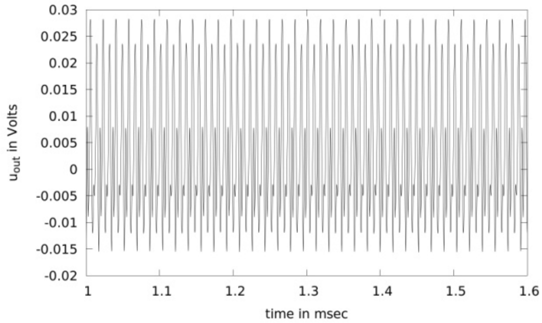

(e)

Fig. 9. Time series for *f* (a) 90 kHz (period-1), (b) 120 kHz (period-2), (c) 140 kHz (period-4), (d) 177 kHz (chaos), (e) 230 kHz (period-4).

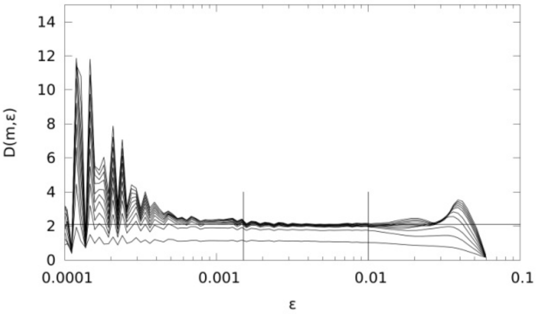

Fig. 10. Local slopes of correlation sums vs. ε . (Embedding dimensions 1-10)

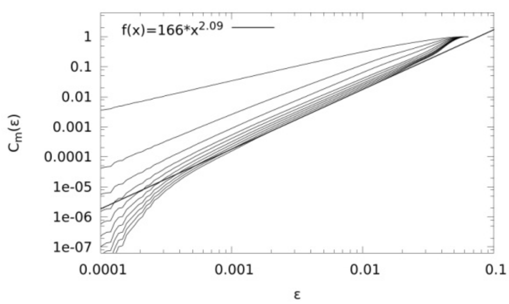

Fig. 11. Correlation sums vs. ε . (Embedding dimensions 1-10)

4. Conclusion

In this work the antimonotonicity phenomenon was studied in the case of a driven R-L-Diode circuit. The substantial number of physical or mechanical systems that exhibit both forward and reverse period doubling cascades motivates the study of this phenomenon. The chosen circuit has a long history of study, because it is one of the experimentally simplest nonlinear circuits that can be constructed. Also, a variety of phenomena related to nonlinear dynamics and chaos has been observed with this circuit. However, in this work our investigation was focused on the antimonotonicity phenomenon, which this circuit presents, as the frequency of the sinusoidal source increases, when the circuit has (or not) a DC bias voltage (V_{DC}). This experimental investigation has not been previously presented in literature and interesting phenomena has been reported for the first time.

Experimental bifurcation diagrams of the voltage across the resistor (V_{out}) versus the frequency (f), with or without a DC bias voltage was captured. From these diagrams a complex bubbling process, including forward and reverse pitchforks was displayed. Having as control parameter of the system the input amplitude (V_{in}) or the DC bias voltage respectively, the dynamic behavior of the system is investigated through bifurcation diagrams in two cases: a) By changing the input amplitude (V_{in}) without DC bias voltage and b) by changing the value of bias voltage when the input sinusoidal signal has a DC component. In both cases a series of forward and inverse bifurcations occur in frequency bands, which increase with the increasing of the amplitude (V_{in}) or the bias voltage (V_d) respectively.

Also, phenomena related to nonlinear dynamics were also observed, such as a tangent bifurcation, which latches the circuit into a period-3 region, and the well-known hysteresis phenomenon. So, our investigation is evidence that homoclinic tangencies were made and broken through a dimple formation process analogously to the process that occurs in other physical systems. Experimental phase portraits of the voltage across the resistor (V_{out}) versus the amplitude (V_{in}) of the voltage source and the respective experimental return maps of $V_{max}(n + 1)$ versus $V_{max}(n)$ confirmed the expected from the bifurcation diagrams circuit's dynamical behavior, while the folding of the attractor in the (υ_{in}, υ_{out})-plane, as the frequency increasing, was also investigated. Also, presence of chaos is verified by calculating a correlation dimension of 2.16. Therefore, this work proves that in addition to the amplitude (V_{in}) or the bias voltage (V_d) dependence of the input sinusoidal signal, which have been studied thoroughly in previous published works, RL-Diode dynamical behavior is also strongly depended on the frequency of the input sinusoidal voltage source. Furthermore, as the amplitude (V_{in}) or the bias voltage (V_{DC}) increased, the frequency range, in which the antimonotonicity phenomenon observed was also increased. In this way, this circuit could operate in higher frequencies, than the most well-known nonlinear circuits, making it capable of using it in real world chaos-based applications, such as encryption, random number generation etc. Also, due to its simple structure and its common elements, this circuit could be a good candidate to be used as a nonlinear circuit for educational purposes.

References

1. B.K. Shivamoggi, Nonlinear Dynamics and Chaotic Phenomena: An Introduction, Springer, 2014.
2. M.P. Kennedy, Three Steps to Chaos, IEEE Trans. Circuits Sys. I, vol. 40, pp. 640-674 (1993).
3. P.S. Linsay, Period Doubling and Chaotic Behavior in a Driven Anharmonic Oscillator, Phys. Rev. Lett., vol. 47, pp. 1349-1352 (1981).
4. R.W. Rollins and E. R. Hunt, Intermittent Transient Chaos at Interior Crises in the Diode Resonator, Phys Rev. A, vol. 29, pp. 3327-3334 (1984).
5. T. Matsumoto, L.O. Chua and R. Tokunaga, Chaos via Torus Breakdown, IEEE Trans. Circuits Sys., vol. 34, pp. 240-253 (1987).
6. C. Jeffries and J. Perez, Direct Observation of Crises of the Chaotic Attractor in a Nonlinear Oscillator, Phys. Rev. A, vol. 27, pp. 601-603 (1983).
7. I.M. Kyprianidis, I.N. Stouboulos, P. Haralabidis and T. Bountis, Antimonotonicity and Chaotic Dynamics in a Fourth Order Autonomous Nonlinear Electric Circuit, Int. J. Bifurcat. & Chaos, vol. 10, pp. 1903-1915 (2000).
8. P.S. Linsay, Period Doubling and Chaotic Behavior in a Driven Anharmonic Oscillator, Phys. Rev. Lett., vol. 47, pp. 1349-1352 (1981).
9. S. Tanaka, S. Higuchi, and T. Matsumoto, Sheet Structure in Global Bifurcations of a Driven R−L-Diode Circuit, Phys. Rev. E, vol. 54, pp. 6014-6028 (1996).
10. J. Milnor and W. Thurston, Iterated Maps of the Interval, Springer, vol. 1342, pp. 465-563 (1988).
11. I. Kan and J. Yorke, Antimonotonicity: Concurrent Creation and Annihilation of Periodic Orbits, Bull. Ann. Math. Soc., vol. 23, pp. 469-476 (1990).
12. S.P. Dawson, C. Grebogi, J.A. Yorke, I. Kan and H. Kocak, Antimonotonicity: Inevitable Reversals of Period-Doubling Cascades, Phys. Lett. A, vol. 162, pp. 249-254 (1992).
13. I. Kan, H. Kocak, and J. A.Yorke, Antimonotonicity: Concurrent Creation and Annihilation of Periodic Orbits, Ann. Math, vol. 136, pp. 219-252 (1992).
14. S.P. Dawson, and C. Grebogi, Cubic Maps as Models of Two Dimensional Antimonotonicity, Chaos Solitons and Fractals, vol. 1, pp. 137-144 (1991).
15. S.P. Dawson, C. Grebogi, and H. Kocak, A Geometric Mechanism for Antimonotonicity in Scalar Maps with Two Critical Points, Phys. Rev. E, vol. 48, p. 1676 (1993).
16. M. Bier, T.C. Bountis, Remerging Feigenbaum Trees in Dynamical Systems, Phys. Lett A, vol. 104(5), pp. 239-244 (1984).
17. G.L. Oppo, A. Politi, Collision of Feigenbaum Cascades, Phys. Rev. A, vol. 30(1), pp. 435-441 (1984).
18. T.C. Newell, P.M. Alsing, A. Gavrielides, and V. Kovanis, Synchronization of Chaotic Resonators Based on Control Theory, Phys. Rev. E, vol. 51, p. 2963 (1995).
19. R. Hegger, H. Kantz, T. Schreiber, Practical Implementation of Nonlinear Time Series Methods: The TISEAN Package*, Chaos*, vol. 9, pp. 413-435 (1999).
20. R.C. Hilborn, Chaos and Nonlinear Dynamics, Oxford University Press, New York, p. 17 (1994).
21. I.M. Kyprianidis, Antimonotonicity in Chua's Canonical Circuit, In. Proc. of the 5th WSEAS Int. Conf. on Non-Linear Analysis, Non-Linear Systems and Chaos, Bucharest, Romania, October 16-18, pp. 75-80 (2006).
22. E. Ott, Chaos in Dynamical Systems, Cambridge University Press, Cambridge, (1993).
23. S.H. Strogatz, Nonlinear Dynamics and Chaos: With Applications to Physics, Biology, Chemistry, and Engineering, Westview Press, (2014).
24. H. Kantz and T. Schreiber, Nonlinear Time Series Analysis, Cambridge: Cambridge University Press, pp. 194-197 (2004).